Combustion and Flame 184 (2017) 233–245

Contents lists available at ScienceDirect

Combustion and Flame

journal homepage: www.elsevier.com/locate/combustflame

Numerical analysis and model development for laminar flame speed of stratified methane/air mixtures

Xian Shi*, Jyh-Yuan Chen

Department of Mechanical Engineering, University of California, Berkeley, Berkeley, CA 94720, USA

ARTICLE INFO

Article history:
Received 4 March 2017
Revised 14 June 2017
Accepted 14 June 2017

Keywords:
Stratified flames
Preferential diffusion
Sensitivity analysis
Flame speed model

ABSTRACT

Numerical simulations of stratified methane/air flames with various stratification configurations are conducted using an 1-D unsteady reacting flow solver. Among all the stratified flame cases investigated, rich-to-lean stratified flames show significant departures from homogeneous flames, i.e., up to 50% increase in fuel consumption speeds, primarily due to preferential diffusion of lighter species and radicals from rich burnt products. A sensitivity study of transport properties further reveals that preferential diffusion of molecular hydrogen H_2 along with radicals H, OH is the dominant factor in increasing stratified flame speeds, compared to the influence of heat diffusion and diffusion of H_2O. Larger departure of stratified flames from homogeneous flames is observed in those cases with higher degree of stratification. In order to model transient behaviors of stratified flames with arbitrary stratification configurations, a local stratification level (LSL) model is proposed. LSL incorporates the effect of preferential diffusion by introducing a transfer function from molecular hydrogen concentration gradients to equivalence ratio gradients, and the memory effect by solving the transient model equation of LSL. The model results match well with directly simulated results quantitatively with error less than ~10% for both lean and rich conditions.

1. Introduction

Stratified combustion exists in a wide range of practical combustion phenomena and industrial applications, from forest wildfires [1], mine gas and vessel ruptures [2,3], to gas turbines and internal combustion (IC) engines [4–6]. Fuel stratification affects a wide range of combustion characteristics from flame speed, autoignition, to even instability. For gas turbines, oscillations in equivalence ratio may trigger thermo-acoustic instabilities in the combustion chamber, which can deteriorate the turbine performance or even cause severe physical damages [7]. In contrast, stratified combustion in direct-injected spark-ignited internal combustion engines has been an effective technique to improve fuel efficiency and reduce emissions [8,9]. Flame propagation speeds of in-cylinder stratified fuel/air mixtures can differ from those of homogeneous mixtures based on local and instantaneous equivalence ratio [10]. Therefore, it is of practical significance as well as fundamental interest to understand the effect of stratification on flame speed. Moreover, an accurate prediction of stratified flame speeds can benefit experiment interpretation and turbulent combustion modeling by developing more comprehensive flame speed look-up tables with consideration of fuel stratification.

There have been several analytical and experimental studies, aiming at understanding the departure of stratified flames from homogeneous flames in terms of flame speed. Karim and Tsang [11] first used a circular pipe filled with two mixtures separated by a plate, where a stratified mixture was formed after removing the separation plate. They found that the flame speeds of a rich-to-stoichiometric methane/air stratified flames were close to the corresponding quasi-homogeneous flame speeds, while the stoichiometric-to-lean stratified flame were ~ 30% faster than the corresponding homogeneous flames. Badr and Karim [12] performed a similar experimental investigation and extended Karim and Tsang's conclusion: stratified flames propagating from mixtures with higher flame speeds to those with lower speeds, e.g., stoichiometric to either lean or rich, were faster than the corresponding homogeneous flames, while stratified flames with opposite directions were close to homogeneous flames. Moreover, the observed stratified flame speeds can be correlated to the homogeneous flame speeds corresponding to fuel concentrations at the ignition point and concentration gradients. However, the correlation was case-specific and valid only under simple stratification cases, where stratification does not change its direction. Around the same time, Mikolaitis [13] performed an asymptotic analysis using exponential scaling of premixed flame propagation with thermal and

* Corresponding author.
E-mail address: xshi@berkeley.edu (X. Shi).

http://dx.doi.org/10.1016/j.combustflame.2017.06.010
0010-2180/

Nomenclature

Greek symbols

δ	Local Stratification Level (LSL)
δ_f	Local Stratification Level (LSL) at flame front
$\dot{\omega}_F$	fuel consumption rate
ϕ	equivalence ratio
ϕ_b	equivalence ratio of burnt mixture
ϕ_f	equivalence ratio at flame front
ϕ_f^b	equivalence ratio at flame front on burnt side
ϕ_f^u	equivalence ratio at flame front on unburnt side
ϕ_u	equivalence ratio of unburnt mixture
T_u	temperature of unburnt mixture

Roman symbols

U	vector of independent variables (governing equation)
$\mathcal{C}$	convection term (LSL model)
$\mathcal{D}$	diffusion term (LSL model)
$\mathcal{R}$	reaction term (LSL model)
C_F	scale constant (LSL model)
$C_{\mathcal{R}}$	reaction constant (LSL model)
C_{grad}	gradient constant (LSL model)
C_{rlx}	relaxation constant (LSL model)
d_f	flame thickness
D_k	diffusivity of species k
d_s	stratification thickness
F	convection term (governing equation)
F_v	diffusion term (governing equation)
Le	Lewis Number
P	pressure
S_c	fuel consumption speed
S_R	chemical source term (governing equation)
T	temperature
t	time
T_b	temperature of burnt mixture
T_u	temperature of unburnt mixture
U	velocity

concentration gradients. The results were restricted to the scenario where the flame preheat zone thickness is very thin and smaller than the length scale of initial temperature or concentration variations. Under this restriction, the author concluded that the flame propagation can be simply determined by the local values of temperature and mixture composition from the initial conditions. As the author pointed out in the paper, such an exponentially thin flame is not of practical significance for most applications. For this reason, Bissett and Reuss [14] adopted a similar approach and obtained a slowly-varying flame with the usual algebraic distance scaling for the flame. They demonstrated that the burning rate of the slowly-varying flame propagating through a region of varying temperature or mixture composition is different from that of corresponding homogeneous flames. In recent years, Kang and Kyritsis [15–17] conducted extensive research on stratified flames, both experimentally and theoretically. They established stratified mixtures through convective-diffusive balance of two methane/air streams in a tube-like burner. Their conclusions were very similar to that of [14] and they pioneered the development of stratified flame speed model. Two different models were proposed: (1) A integrated measure Q model was proposed in [15], where Q is the product of the average equivalence ratio gradient times the ratio of the average over the local value of equivalence ratio. A critical value $Q_0 = 0.018$ mm^{-1} is used to determine whether a stratified flame starts to deviate from its corresponding homogeneous flames. (2) A theoretical model was further proposed [17] on the basis of the hypothesis that stratified flames differ from homogeneous flames due to the effect of cumulative heat support from burnt gas. The model predicted quantitatively well with their experimental results of stoichiometric-to-lean or lean-to-leaner stratified flames but not rich flames. Balusamy et al. [18] performed stratified flame experiments of propane/air in a constant volume chamber, where a rich mixture was ignited and the corresponding flame propagated into lean mixtures. The flame propagation in the lean mixtures was found back-supported by the ignition in richer conditions, as the flame benefited from the rich composition of the burnt gas compared to that of lean homogeneous flames.

In spite of many interesting experimental observations and insights, all the above studies did not study the effect of preferential diffusion, which has been shown to play an important role in hydrocarbon stratified flames by many numerical studies [19–21]. For example, in a rich-to-lean stratified methane/air flames, rich flames can generate a significant amount of molecular hydrogen which diffuses faster than the flame front so that the excess hydrogen can penetrate into unburnt mixtures. A corresponding enhancement in flame speeds is thereby observed. As Kang and Kyritsis [17] pointed out in their latter model, the reason why the model did not work in rich flames was probably due to the single-step-chemistry approximation which did not include hydrogen as an intermediate species.

This paper examines the effect of preferential diffusion on the enhancement of flame speed with a detailed quantitative analysis, including a sensitivity study of transport properties. Furthermore, to the best of the authors' knowledge, there does not exist a stratified flame speed model that takes into account of differential diffusion and covers a wide range of conditions, both rich and lean. In order to improve current understanding of stratified flames and to facilitate development of stratified flame speed models, this paper

1. presents detailed one-dimensional stratified flame numerical results of methane/air flames with mixture-average diffusivity model and validated reduced chemical kinetic model;
2. discusses various stratification configurations of stratified methane/air flames;
3. conducts a sensitivity study of diffusivities to identify the root cause for the difference between laminar flame speeds of stratified and homogeneous mixtures;
4. proposes a transient local stratification level (LSL) model incorporating both the effect of preferential diffusion and the memory effect.

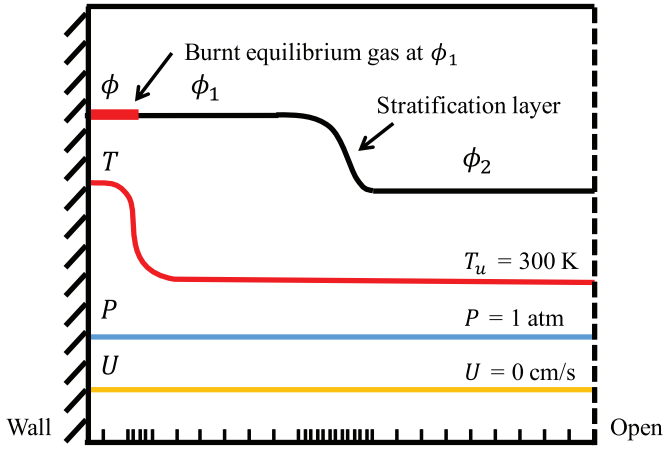

Fig. 1. Schematic of stratified flame propagating from unburnt mixture of ϕ_1 to that of ϕ_2 in 1-D planar coordinate.

Details of numerical setup and definitions of key flame characteristics are elaborated first. Stratified and homogeneous flame simulation results are presented in the sequence of (1) detailed comparisons between flame structures and profiles of stratified and homogeneous flames, (2) a sensitivity analysis of transport properties and (3) the LSL model including model approach, development and assessment.

2. Numerical model and setup

ASURF-Parallel [22], a parallel version of the Adaptive Simulation of Unsteady Reacting Flow [23,24], is used to perform transient simulations of stratified and homogeneous flames. A general form of the governing equations is as below

$$\frac{\partial \mathbf{U}}{\partial t} + \frac{\partial F(\mathbf{U})}{\partial x} = \frac{\partial F_v(\mathbf{U})}{\partial x} + S_R(\mathbf{U}), \tag{1}$$

where the four vectors $\mathbf{U}$, $F(\mathbf{U})$, $F_v(\mathbf{U})$, $S_R(\mathbf{U})$, i.e., unsteady term, convection term, diffusion term, chemical source term, are defined as:

$$\mathbf{U} = \begin{pmatrix} \rho Y_1 \\ \rho Y_2 \\ \vdots \\ \rho Y_N \\ \rho u \\ E \end{pmatrix} \quad F(\mathbf{U}) = \begin{pmatrix} \rho u Y_1 \\ \rho u Y_2 \\ \vdots \\ \rho u Y_N \\ \rho u^2 + P \\ (E+P)u \end{pmatrix}$$
$$F_v(\mathbf{U}) = \begin{pmatrix} -\rho u Y_1 V_1' \\ -\rho u Y_2 V_2' \\ \vdots \\ -\rho u Y_N V_N' \\ \tau \\ q + \Phi \end{pmatrix} \quad S_R(\mathbf{U}) = \begin{pmatrix} \omega_1 \\ \omega_2 \\ \vdots \\ \omega_N \\ 0 \\ 0 \end{pmatrix} \tag{2}$$

In total, N+2 equations are solved including conversation equations of N species, momentum, and energy. In the species conservation equations, N is the total number of species, ρ is the mixture density, and Y_k, V_k', ω_k are the mass fraction, diffusion velocity and production rate of species k, respectively. V_k' is calculated using a mixture-average diffusivity model provided by the TRANSPORT library [25]. In addition, the thermal diffusion of H and H_2 is also considered and a correction velocity is added to ensure mass conservation [25]. ω_k is calculated using a chemical kinetic model, which will be introduced later, through the CHEMKIN library [26]. In the momentum equation, P is the hydro-static pressure and τ is the viscous stress,

$$\tau = \frac{4}{3}\mu \frac{\partial u}{\partial x}, \tag{3}$$

where μ is the mixture viscosity. In the energy equation, E is the total energy,

$$E = -P + \frac{\rho u^2}{2} + \rho \sum_{k=1}^{N} (Y_k h_k), \tag{4}$$

where h_k is the enthalpy of species k. q is heat flux while Φ is the viscous dissipation,

$$q = \lambda \frac{\partial T}{\partial x} - \rho \sum_{k=1}^{N} (Y_k h_k V_k'), \tag{5}$$

$$\Phi = u \frac{\partial \tau}{\partial x} + \frac{4}{3}\mu \left(\frac{\partial u}{\partial x} \right)^2, \tag{6}$$

where λ is the mixture thermal conductivity.

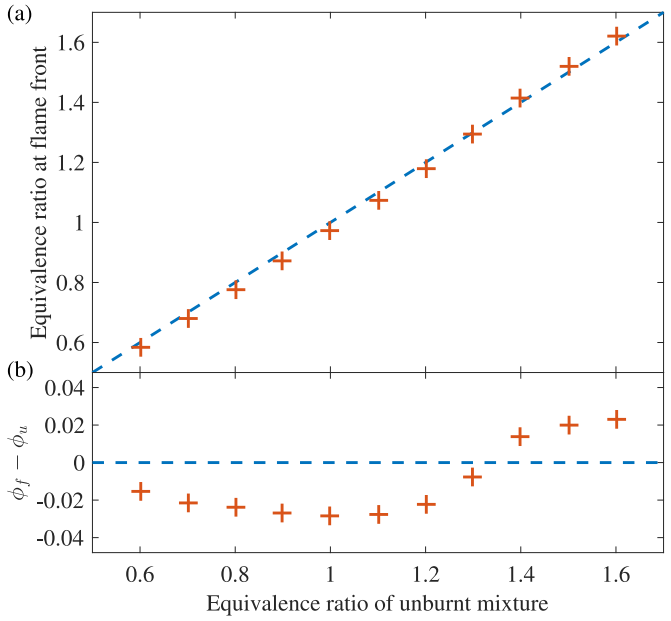

Fig. 2. (a) Equivalence ratio of unburnt mixture (ϕ_u) and equivalence ratio at flame front (ϕ_f), and (b) their differences, of methane/air homogeneous flames.

For the time integration of these governing equations, a second-order Strang Splitting method is used to decouple the calculations of different physical processes: For the ordinary differential equations of chemical system, the implicit VODE solver is used. For the partial differential equations of convection and diffusion processes, a second-order TVD Runge–Kutta method is used, where convection is calculated using MUSCL-HANCOCK Scheme and diffusion using central difference scheme.

A schematic of one example stratified flame is shown in Fig. 1. The length of the entire calculation domain is 20 cm. Reflective boundary condition (wall) is imposed on the left end, while zero-gradient boundary condition (open) is imposed on the right. A 7-level adaptive mesh refinement scheme is implemented with the minimum grid size 4 μm to resolve both the flame front and the stratification layer. The flame is initialized near the left wall using the temperature and mixture composition of burnt equilibrium gas of equivalence ratio ϕ_1. A stratification layer where the equivalence ratio of the mixture transitions from ϕ_1 to ϕ_2 is placed at a distance away from the initial flame. By changing the distance between the initial flame front and the stratification layer, different degrees of initial stratification can be achieved. The initial temperature, pressure and fluid velocity fields of unburnt gases are set to 300 K, 1 atm, and 0 cm/s, respectively.

A 16-species reduced chemical kinetic model [21] was developed from a small version of GRI 3.0 [27] model without NO_X chemistry. The computed flame speeds of homogeneous flames agree well with experimental data available in the literature and the comparisons are included in the supplemental materials.

3. Flame characteristics

3.1. Equivalence ratio

The conventional definition of equivalence ratio, i.e., the ratio of the fuel/air ratio to the stoichiometric fuel/air ratio, is suitable for unburnt mixtures where fuel and air are unanimously defined. However, this definition is not applicable to the instantaneous mixtures within the flame zone due to two issues. First, fuel and oxidizer may have reacted into intermediate species so that the equiv-

alence ratio can no longer be calculated based on fuel and air only. Second, differential diffusion of species alters the mixture compositions across the flame zone. Note that both issues exist in both stratified and homogeneous flames. For a homogeneous flame, its equivalence ratio can be uniquely defined using the unburnt mixture. In contrast, stratified flames are more complicated in the absence of a unique unburnt mixture.

In this study, the reference equivalence ratio is defined on the basis of the element composition of hydrocarbon/air systems:

$$\phi = \frac{X_H + 4X_C}{2X_O}, \tag{7}$$

where X_H, X_C and X_O denote the mole fractions of elements H, C and O, respectively. Figure 2 shows the computed equivalence ratios of a series of methane/air homogeneous flames with unburnt temperature at 300 K and pressure at 1 atm. Each point represents one specific homogeneous flame and ϕ_u refers to the equivalence ratio calculated based on the element composition of unburnt mixture while ϕ_f is based on the element composition at flame front. The location of maximum heat release rate is referred to as the flame front. The difference between ϕ_u and ϕ_f is shown in the lower part of the figure. Due to differential diffusion, ϕ_u and ϕ_f can differ up to 0.04 in methane/air homogeneous flames under ambient conditions. For consistent comparisons between stratified and homogeneous flames, Eq. (7) will be used for computing the equivalence ratios.

3.2. Laminar flame speed

Fuel consumption speed, S_c, is used in this study as the reference laminar flame speed. S_c can be derived from the flame property profiles and frequently used in numerical simulations. In this study, S_c is derived from the mass balance of a stationary flame and written as [28]:

$$S_c = -\frac{1}{\rho_u Y_F^u}\int_{-\infty}^{+\infty} \dot{\omega}_F dx, \tag{8}$$

where ρ_u is the unburnt density, Y_F^u is the mass fraction of fuel species in the unburnt mixture, and $\dot{\omega}_F$ is the fuel consumption rate. In the denominator, Y_F^u is used instead of $Y_F^u - Y_F^b$ which was used in the original theoretical derivation, due to uncertainty in determining Y_F^b in propagating flames.

3.3. Flame thickness, stratification gradient and thickness

Figure 3 presents the computed temperature and equivalence ratio profiles of both (a) a homogeneous flame and (b) a stratified flame, where $x = 0$ denotes the location of the flame front. The region $x > 0$ corresponds to the unburnt mixture. For the homogeneous flame, ϕ_u is 1.00. For the stratified flame, the flame experiences an equivalence ratio change from $\phi_u = 1.6$ to 0.6. At the flame front of this particular moment, the equivalence ratio, ϕ_f, of both flames is 0.97. As seen in Fig. 3, these two flames have similar temperature profiles. In Fig. 3(b), the stratified flame experiences a decreasing profile of equivalence ratio as it propagates from a rich mixture into a lean mixture. The flame thickness can be calculated on the basis of temperatures by the following equation [29],

$$d_f = \frac{T_b - T_u}{\left|\frac{dT}{dx}\right|_{max}}. \tag{9}$$

In this study, the flame thicknesses of homogeneous flames ranges from 0.05 to 0.1 cm. Based on d_f, the instantaneous equivalence ratio gradient at the flame front can be approximated by

$$\frac{d\phi}{dx} = \frac{\phi_f^b - \phi_f^u}{d_f}, \tag{10}$$

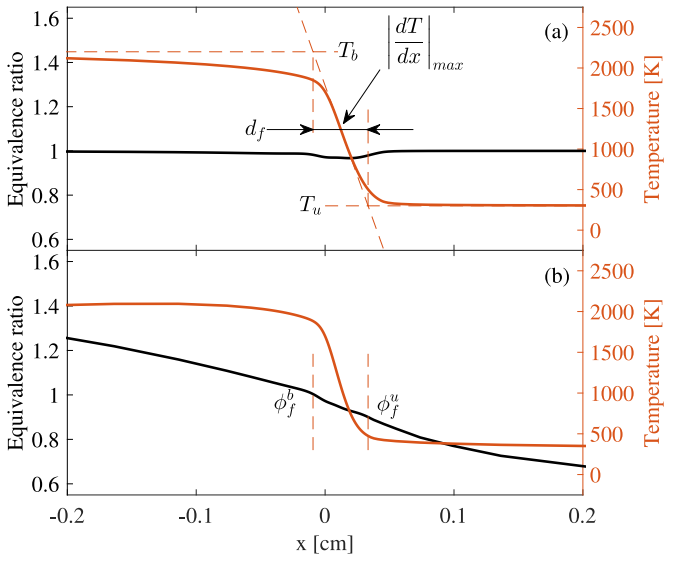

Fig. 3. Equivalence ratio and temperature profiles of (a) a homogeneous flame and (b) a rich-to-lean stratified flame, $\phi_f = 0.97$.

where ϕ_f^u and ϕ_f^b denote the equivalence ratios at the boundaries of flame zone. As d_f changes with flame dynamics, equivalence ratio gradient at flame front is a transient property of a propagating flame and it can be evaluated instantaneously. The equivalence ratio gradient at flame front is used to describe the instantaneous stratification conditions when the flame front passes through the stratification layer and therefore a key parameter in stratified flame speed models.

To quantify the degree of initial stratification in different stratified configurations, stratification thickness d_s is defined as

$$d_s = \frac{|\phi_2 - \phi_1|}{\left|\frac{d\phi}{dx}\right|_{u,max}}. \tag{11}$$

In the case of stratified flames propagating from unburnt mixture ϕ_1 to ϕ_2. d_s is calculated when the flame front in stratified flames reaches the stratification layer as shown in Fig. 4. Therefore d_s is based on equivalence ratio of unburnt mixtures and therefore least affected by differential diffusion. For all the stratified flame cases investigated in this study, the stratification thickness is kept

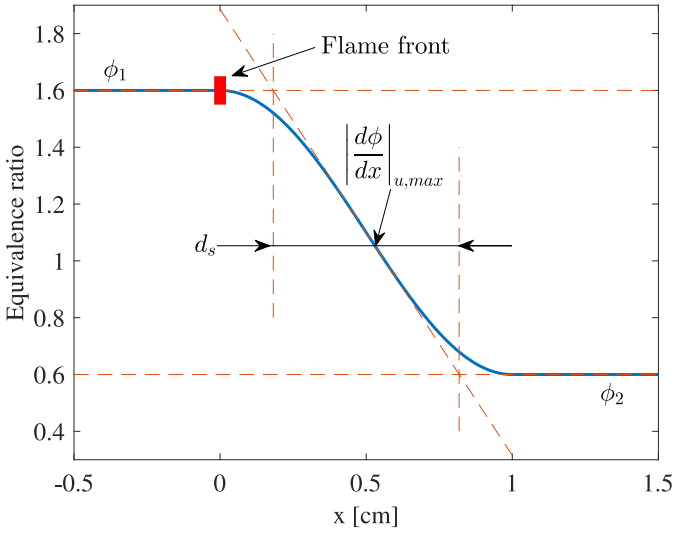

Fig. 4. Schematic of stratification thickness calculation in the rich-to-lean stratified flame propagating from $\phi_u = 1.6$ to 0.6.

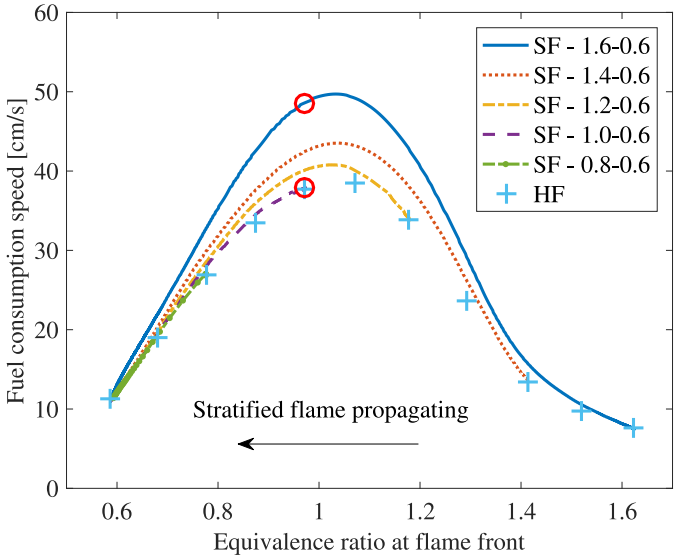

Fig. 5. Fuel consumption speeds of SF propagating into lean mixtures and corresponding HF.

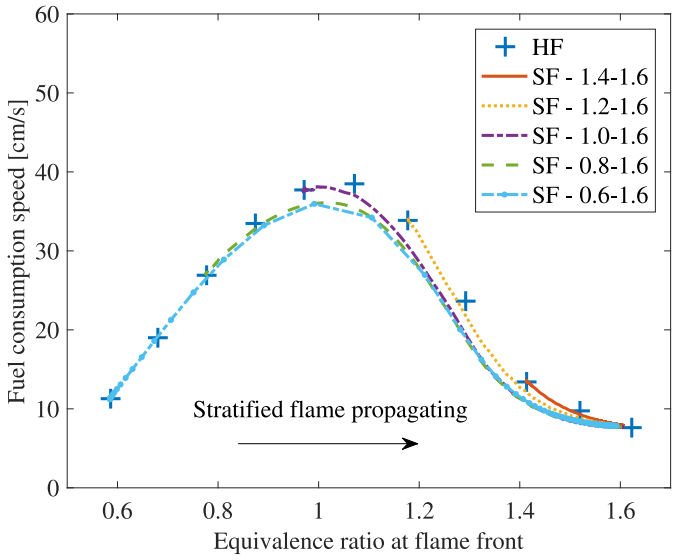

Fig. 6. Fuel consumption speeds of SF propagating into rich mixtures and corresponding HF.

on the order of 0.1 cm if not specified otherwise. The location of this stratified layer from the initial flame can be altered, resulting in a change of the stratification thickness when the flame approaches the layer.

Cases are run with a range of stratification thicknesses, which are either on the same order of or larger than the flame thickness. These runs intend to simulate stratified flames in the wrinkled flame regime, which is observed in many practical devices, such as a direct injection IC engine. The stratification in such an engine is mainly dominated by the turbulence smallest length which is normally larger than the flame thickness.

4. Results and discussion

A series of stratified flames (SF) is first compared to their corresponding homogeneous flames (HF). In order to identify the root cause for the differences between SF an HF, detailed flame property profiles of representative SF and HF, as well as a sensitivity analysis of transport properties, are conducted.

4.1. Comparison between stratified and homogeneous flames

Figure 5 presents the computed fuel consumption speeds of five SF propagating from unburnt mixtures of $\phi_u = 1.6, 1.4, 1.2, 1.0, 0.8$ into an unburnt mixture of $\phi_u = 0.6$, and the corresponding HF. The computed flame speeds are plotted against equivalence ratio at flame front ϕ_f. Similarly, Fig. 6 shows the results of five SF propagating from unburnt mixtures of $\phi_u = 0.6, 0.8, 1.0, 1.2, 1.4$ into an unburnt mixture of $\phi_u = 1.6$ as well as HF. The stratification thicknesses of all the SF cases shown in Figs. 5 and6 are on the order of 0.1 cm. While fuel consumption speeds of most SF cases are very close to those of HF for lean-to-rich SF, the rich-to-lean SF, e.g., 1.6–0.6 and 1.4–0.6 SF, show significant departures from HF, with up to 30% increase in fuel consumption speeds.

To reveal the underlying physics causing such large departures, detailed flame property profiles of the 1.6–0.6 SF and HF at $\phi_f = 0.97$ (marked by circles in Fig. 5) are analyzed, where a significant difference in fuel consumption speeds is observed ($S_{c,HF} = 37.8$ cm/s, $S_{c,SF} = 48.5$ cm/s). Figure 7 compares the computed profiles of heat release rate and temperature in the flame front frame of reference, where $x = 0$ denotes the flame front location, with the unburnt mixture on the right and the burnt mixture on the left. As

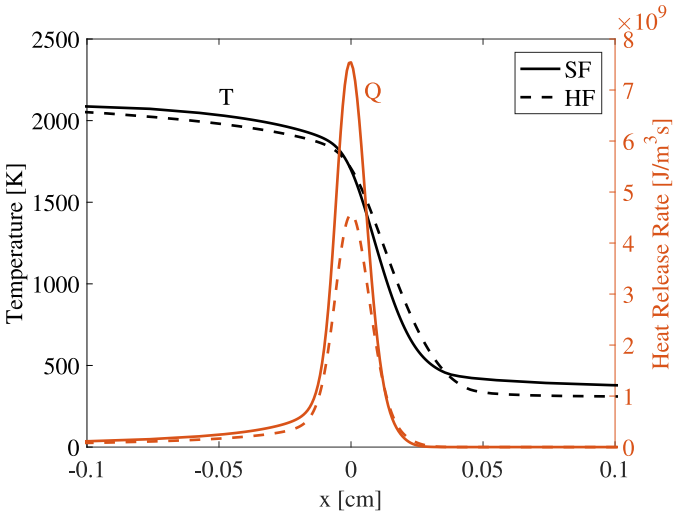

Fig. 7. Heat release rate and temperature profiles of 1.6–0.6 SF and HF, $\phi_f = 0.97$.

seen in the figure, the heat release rate of SF is significantly higher ($\sim$ 60%) than that of HF near the flame front, which is consistent with the observed flame speed enhancement. In terms of temperature, SF and HF are very similar: on the burnt side, the temperature of SF is slightly higher than that of HF due to a higher heat release rate. For the region $x > 0.04$ cm, the unburnt temperature of SF is seen higher than that of HF by $\sim$ 50 K. Since there is negligible heat release in the unburnt mixture of SF, the temperature rise is caused by transport processes, i.e., either heat diffusion or mass diffusion carrying extra enthalpy.

Figure 8 shows the profiles of reactants CH_4, O_2 and products H_2O, CO_2 for both SF and HF. The decreasing profile of CH_4 in the unburnt mixture of SF ($x > 0.04$ cm) is indicative of that SF propagates into a leaner mixture. On the burnt side ($x < 0$), SF has much more H_2O but less CO_2. On the unburnt side, SF also has more H_2O, similar to the temperature profile comparison. Since H_2O has a smaller molecular mass compared to other major product species, preferential diffusion of H_2O leads to more H_2O diffusing into the unburnt mixture. Figure 9 compares the profiles of intermediate species CO, H_2 and radical H, OH, while Fig. 10 compares the production rates of H_2, H and OH. The production rate

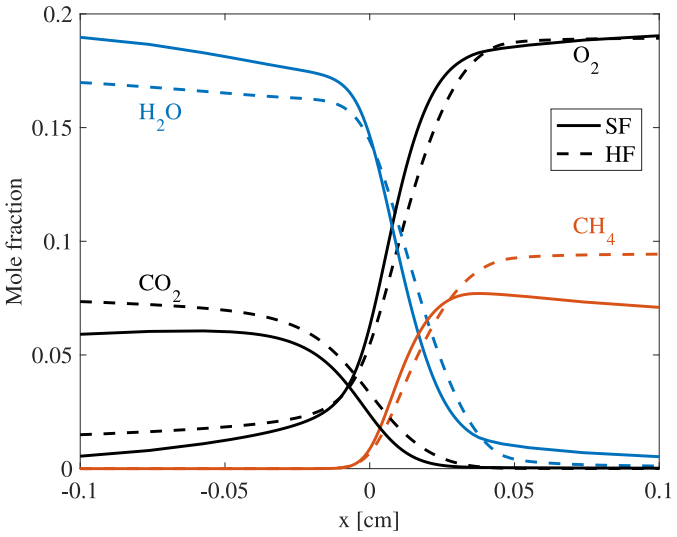

Fig. 8. Reactant and product profiles of 1.6–0.6 SF and HF, $\phi_f = 0.97$.

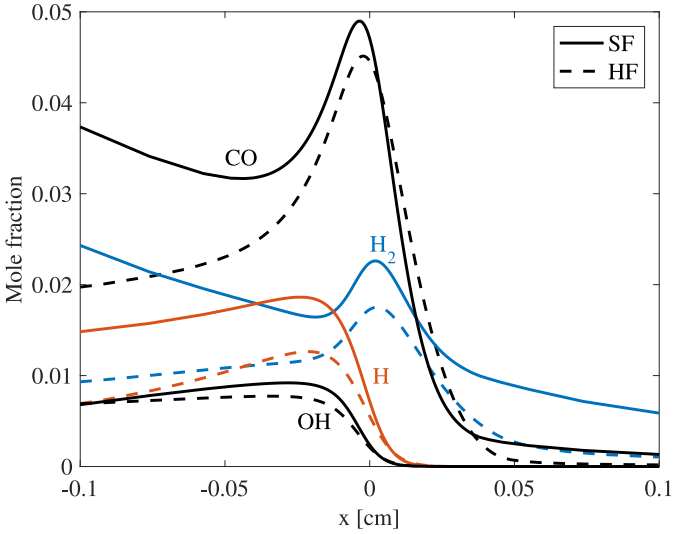

Fig. 9. Major intermediate species and radical profiles of 1.6–0.6 SF and HF, $\phi_f = 0.97$.

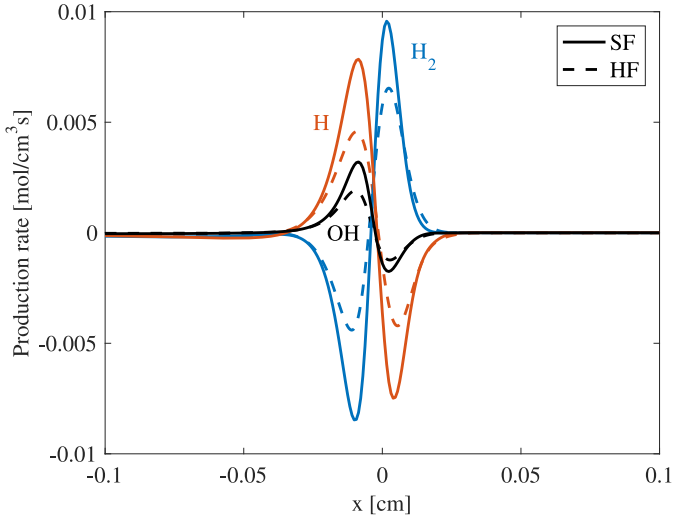

Fig. 10. Production rate profiles H_2, H and OH, of 1.6–0.6 SF and HF, $\phi_f = 0.97$.

profile of CO is very similar to that of H_2, thus not shown. Relative to the HF, all these species have higher concentrations near the flame front in SF, as well as higher production rates. In particular, the concentration of H_2 in SF is much higher than HF, not only near the flame front, but also on both burnt and unburnt sides. As the SF propagates from rich mixtures, excess fuel decomposes and produces extra H_2 in the burnt products. As an extremely light species with small molecular mass, H_2 is able to diffuse much faster than most other species as well as the flame front propagation [22]. Consequently, the extra H_2 in the rich burnt products diffuses into the flame front as well as the unburnt mixture. The enhanced level of H_2 not only boosts flame speed by producing more H and OH radicals as indicated in Fig. 10, but also increases the temperature of unburnt mixtures and generates even more H_2. This also explains that SF produces more H_2O but not CO_2 compared to HF. To summarize, the increase in flame speeds of rich-to-lean SF is found closely related to the preferential diffusion of lighter species, such as H_2O and H_2.

4.2. Sensitivity study of transport properties

Although the detailed analysis of flame properties has revealed the key differences between SF and HF, the relative contributions from various transport processes, such as heat transfer, mass diffusion of different species, need to be clarified. To evaluate the relative importance of these transport processes, a sensitivity study of thermal and mass diffusivities on the computed flame speeds is conducted. Figure 11 compares the fuel consumption speeds of the 1.6–0.6 SF and HF under four different scenarios of transport properties. In Fig. 11(a), the assumption of unity Lewis number (unity-Le) is made for all species, i.e., the diffusivity of every species is set equal to the thermal diffusivity of the bulk fluid. The computed flame speeds of HF drop by $\sim$ 30% compared to those without the assumption of unity Lewis number, i.e., the results in Fig. 11(d). Furthermore, the computed flame speeds of SF and HF are very close to each other with the maximum difference less than 5%. Since the effect of differential diffusion is eliminated by the unity-Le assumption, the differences between SF and HF are caused by both heat and mass diffusion. Through the stratification layer, the instantaneous adiabatic flame temperature varies according to the varying mixture composition at the flame front, so do the distributions of intermediate species and radicals. Therefore, SF flame front still experiences either back- or front-support heat and mass diffusion [16,30]. However, the unity-Le result suggests that the effect of heat and mass diffusion processes without differential diffusion is very weak in the methane SF.

If the unity-Le assumption is only applied to lighter species H_2, H_2O, H and OH, the computed results shown in Fig. 11(b) are only slightly different from those in Fig. 11(a). In Fig. 11(c), the unity-Le assumption is made only to H_2 and H_2O. A significant increase in the computed flame speeds is observed in both SF and HF, while a clear difference between SF and HF appears. These results imply that the preferential diffusion of radicals H and OH not only plays an important role in HF, but also contributes to the enhancement observed in SF. Compared to Fig. 11(c), the HF results without the unity-Le assumption in Fig. 11(d) are almost identical; however, an even larger difference between SF and HF is observed. To summarize, the enhancement of flame speeds in SF mainly comes from the preferential diffusion of lighter immediate species and radicals.

As H_2 and H_2O in SF are capable of diffusing preferentially into unburnt mixtures and causing an increase in unburnt temperature, the reaction rates as well as flame temperatures may increase correspondingly. Numerical experiments are conducted with enhanced or reduced diffusivities of H_2 and H_2O by 50%. Figure 12 shows the sensitivity of computed results with respect to the dif-

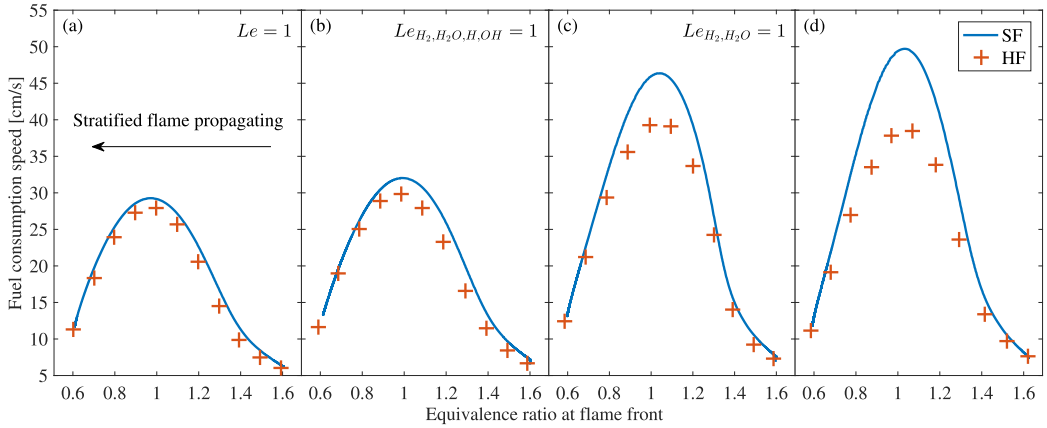

Fig. 11. Fuel consumption speeds of 1.6–0.6 SF and HF with different assumptions of unity Lewis number: (a) $Le = 1$, (b) $Le_{H_2,H_2O,H,OH} = 1$, (c) $Le_{H_2,H_2O} = 1$, (d) no unity-Le assumption.

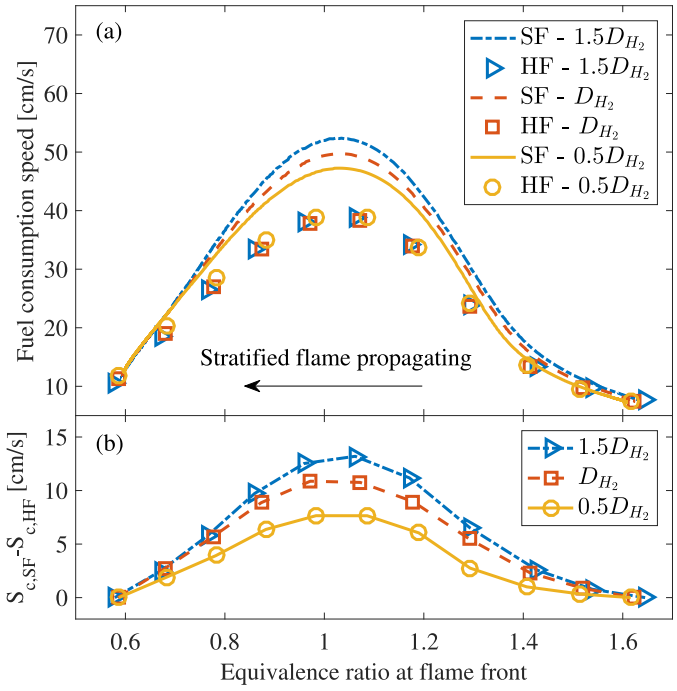

Fig. 12. (a) Fuel consumption speeds of 1.6–0.6 SF and HF, and (b) the respective differences between SF and HF, with different diffusivity of H_2.

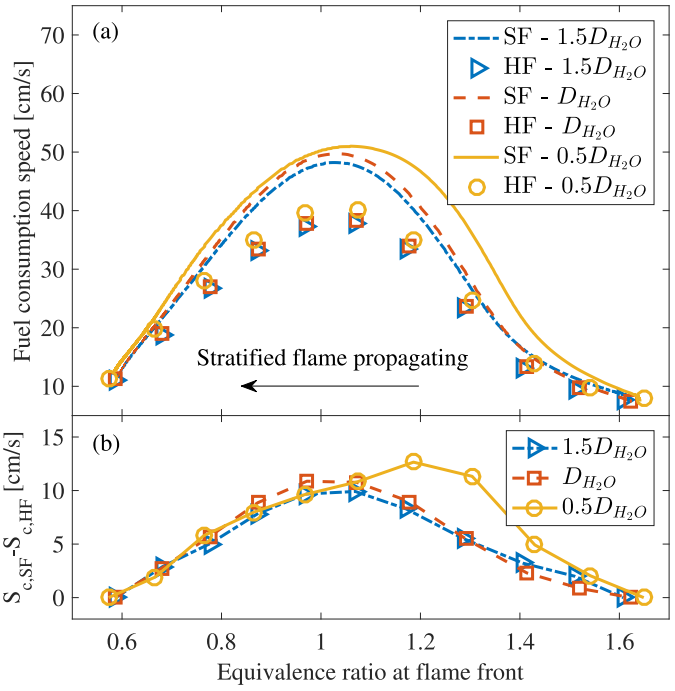

Fig. 13. (a) Fuel consumption speeds of 1.6–0.6 SF and HF, and (b) the respective differences between SF and HF, with different diffusivity of H_2O.

fusivity of H_2. While the flame speeds of HF with three different diffusivity values are almost the same, the differences between SF and HF increase with enhanced H_2 diffusivity. This is expected as more H_2 diffuse from the burnt zone toward the flame front leading to an enhanced reactivity of the flame front by producing more radicals. In comparison, Fig. 13 shows the corresponding results when the diffusivity of H_2O is altered. With higher diffusivity value of H_2O, the difference between SF and HF reduces implying that preferential diffusion of H_2O decreases the reactivity of SF. By comparing the detailed flame profiles, slightly higher unburnt temperature, more H_2O but slower chemical kinetics are observed in the unburnt mixture near flame front with a higher H_2O diffusivity. Therefore, the dilution/quenching effect introduced by H_2O outplays its enthalpy-carrying benefit.

In conclusion, the preferential diffusion of H_2 along with radicals H and OH is found to play an influential factor in stratified flames. Unlike short-lived radicals H and OH, a noticeable amount of H_2 can be produced from rich methane/air flames. On one hand, H_2 as a very reactive species, produces key chain-branching radicals, such as H and OH, leading to higher heat release rates and consequent higher flame speeds. On the other hand, extra H_2 diffuses from the burnt zone into the unburnt mixture and increases the unburnt temperature, which also results in higher reaction rates.

The methodology of this sensitivity study can be applied to heavier fuel species or different diluent scenarios. As shown in the previous study [21], rich flames of heavier fuel species, such as propane and n-heptane, have more complicated chemical pathways than those of methane. In particular, some small intermediate hydrocarbon molecules also play a role in causing the differences between flame speeds of SF and HF. Therefore, sensitivity studies under such scenarios need to include a wider range of species and radicals.

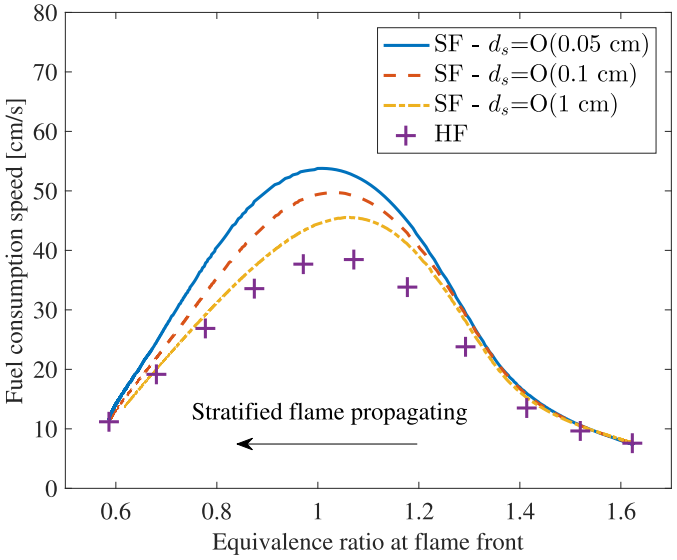

Fig. 14. Fuel consumption speeds of 1.6–0.6 SF with different stratification thicknesses and HF.

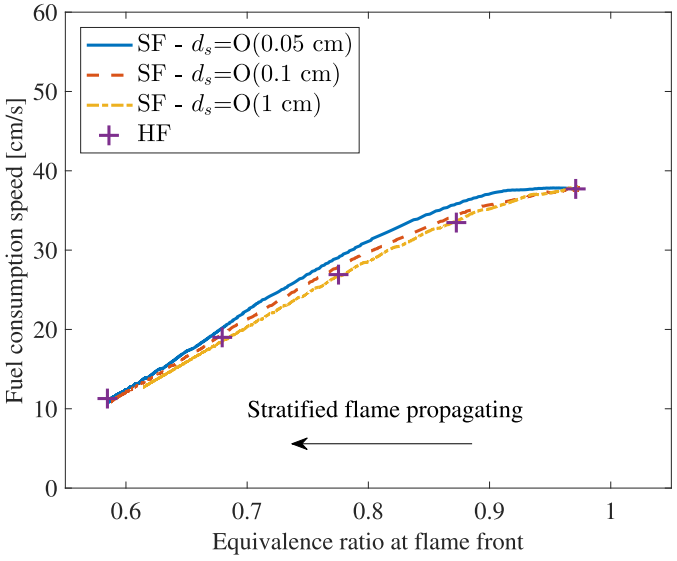

Fig. 15. Fuel consumption speeds of 1.0–0.6 SF with different stratification thicknesses and HF.

4.3. Effect of stratification thickness and equivalence ratio gradient

Although the main cause of SF to differ from HF is tied to preferential diffusion, correlations between the degree of stratification and departure of SF from HF are needed for development of stratified flame speed models. To this end, several cases of SF with different initial stratification thicknesses, determined by Eq. (11), are computed. Figure 14 shows the results of three 1.6–0.6 SF compared to HF. As expected, a stratification layer with a smaller thickness results in a larger gradient of H_2 in the burnt products leading to stronger enhancement in SF, up to 50% increase in the d_s = O(0.05 cm) case. In comparison, Fig. 15 shows the results of three 1.0–0.6 SF compared to HF. As the stoichiometric methane/air flame does not produce as much hydrogen in the burnt products, even with the smallest stratification thickness, the enhancement in SF is noticeable but insignificant. Therefore, the difference in the flame speeds between SF and HF depends on the

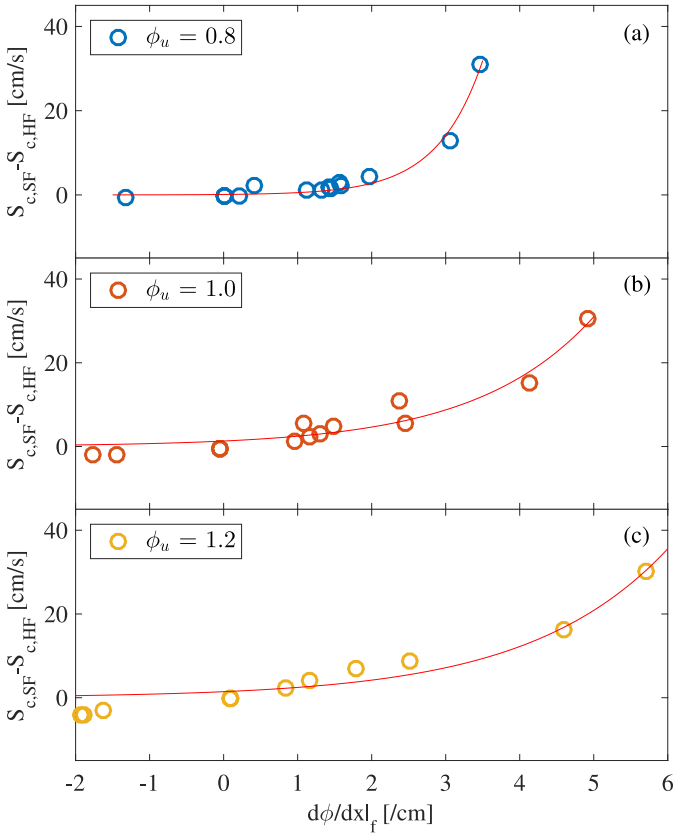

Fig. 16. Departure of fuel consumption speeds of stratified flames compared to homogeneous flames based on instantaneous equivalence ratio gradients at flame front: (a) ϕ_u = 0.8, (b) ϕ_u = 1.0, (c) ϕ_u = 1.2.

degrees of stratification as well as the availability of H_2 in burnt gases.

Besides the initial stratification thickness, the instantaneous equivalence ratio gradients at the flame front, calculated by Eq. (10), is also a useful parameter to correlate the differences between SF and HF when the SF burns through the stratified layer. Figure 16 shows the results of stratified flames at ϕ_u = 0.8, 1.0 and 1.2 from different initial stratification setups. The points are taken from the simulations presented in Figs. 5 and6, as well as simulations of same configurations but with different stratification thicknesses. A positive correlation can be seen between the instantaneous equivalence ratio gradient and the difference between SF and HF. The deviation from a linear line shows that the instantaneous equivalence ratio alone is insufficient to describe the flame speed mainly due to the memory effect. In addition, all the stratified flames simulated so far are ideal and monotonic cases, where the flame monotonically propagates from one mixture into another. A simple correlation may not hold for more complicated and non-monotonic stratified flame configurations. For example, in a 3-phase rich-lean-rich methane/air stratified flame case (which will be shown later in the model section), when the flame front passes through the leanest condition, the flame front is at the minimum value of equivalence ratios. Although the instantaneous equivalence ratio gradient is thus zero, the computed flame speed of the SF is still higher than that of HF due to memory effect that the SF propagates from rich mixtures with excess of H_2. In stratified turbulent flames, the flame front may often experience such non-monotonic variations of equivalence ratios. In those cases, the memory effect of stratified flame makes the equivalence ratio gradient alone insufficient to describe the stratified flames. The above

observation is consistent with the importance of memory effect recognized by many previous studies [14,16,18,31,32].

4.4. Model development for laminar flame speed of stratified methane/air mixtures

The goal of a stratified flame speed model is to accurately describe stratified flame speeds by distinct flame features. With a reasonably accurate flame speed model, stratified flames can be simulated without time-consuming computations of detailed chemistry and multi-component transports. Such a model can be implemented in the G-equation method or other level-set methods, where flame speed tables are used [33]. In terms of modeling methodology, there are two general approaches to incorporate the memory effect. The first approach is to calculate model variables based on information from previous flame front locations, while all the required information are taken under the current time step. For example, Kang and Kyritsis [15] used the integral (global) characteristics of the equivalence ratio distribution and proposed a corrected overall equivalence ratio gradient to evaluate stratified flames. Although this approach is of mathematical convenience and easy to implement, it has several major disadvantages. First, the model only works qualitatively for specific situations, e.g., monotonic stratification layers. Second, it becomes very difficult to implement the model in multidimensional simulations due to the ambiguity of flame propagation direction and trajectory.

The second approach is to construct a transient model variable and solve for the corresponding modeling equation. The model variable can be then evaluated on-the-fly or post-processed. As such, the model is able to carry the accumulated information (memory effect) when appropriately constructed. This approach is based on fluid equations and chemical processes, and can be directly implemented in multidimensional simulations. To this end, δ, defined as local stratification level (LSL), is proposed as the key variable to represent the departure of SF from HF. Specifically, the LSL at flame front, denoted by δ_f, is evaluated and correlated to the difference between fuel consumption speeds of SF and HF. There are essentially two steps involved in this modeling approach:

- Step 1: Construct and solve for a model equation of δ_f, based on global characteristics of stratified flames.
- Step 2: Correlate δ_f to the difference between the flame speeds of SF and HF.

During Step 1, in order to construct the model equation of δ_f, δ is assumed to relate to one or more instantaneous flame properties, such as flame temperature and concentration of certain species. Although there are many ways to relate δ to any combination of flame properties, the difference between the amounts of H_2 of SF and HF seems to be a reasonable choice based on the analysis presented above. Figure 17 shows the positive correlation between flame speed differences and the differences between mole fraction of H_2 on the unburnt side, i.e., $X^u_{H_2,f}$, of SF and HF. $X^u_{H_2,f}$ refers to the amount of H_2 at the location of ϕ^u_f in Fig. 3. The points are taken from all the computed stratified and homogeneous flames presented in this paper. An overall linear correlation is observed and provides some justification that the difference in the molecular hydrogen between SF and HF is a reasonable candidate for constructing δ.

A control volume surrounding δ_f is sketched in Fig. 18. Since δ_f is the LSL at flame front, the control volume moves along with the flame implying that a flame front tracking method is required. The control volume illustrates the physical processes which drive the change of δ_f and facilitates a simplified model. Instead of solving the entire field of δ, the change of δ_f can be simply modeled by considering (1) diffusion, (2) convection and (3) chemical reactions as described in Eq. (12). As H_2 is an intermediate species for methane/air flames, both its concentration and the concentration gradient on the unburnt side are assumed to be zero.

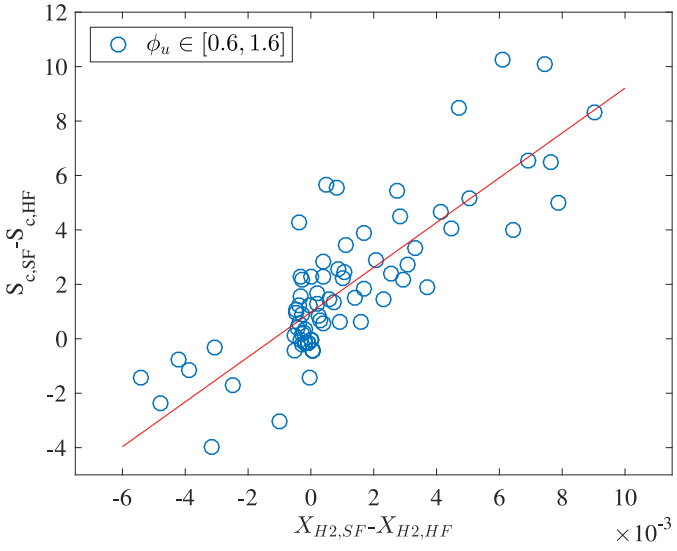

Fig. 17. Correlation: difference between flame speeds of SF and HF, versus difference between mole fractions of H_2 on the unburnt side of SF and HF flame fronts.

$$\frac{d\delta_f}{dt} = \mathcal{D} + \mathcal{C} + \mathcal{R} \tag{12}$$

The diffusion process is assumed to obey the Fick's law and the gradient of δ is correlated to local equivalence ratio and its gradient:

$$\mathcal{D} \approx D_{km}\left.\frac{d^2\delta}{dx^2}\right|_f \approx C_{\mathcal{D}} D_{km} \frac{\left.\frac{d\delta}{dx}\right|_b - 0}{d_f}$$
$$\approx C_{\mathcal{D}} \frac{D_{km}}{d_f}\left.\frac{d\delta}{dx}\right|_f \approx C_{\mathcal{D}} \frac{D_{km}}{d_f} f(\phi)\left.\frac{d\phi}{dx}\right|_f, \tag{13}$$

where

$$\left.\frac{d\delta}{dx}\right|_f \approx f(\phi)\left.\frac{d\phi}{dx}\right|_f.$$

The subscript b denotes the quantity on the burnt side of the control volume and $f(\phi)$ denotes the transfer function from gradient of δ to equivalence ratio gradient at flame front. The transfer function is assumed to be a function depending only on ϕ, as the local concentration of H_2 is primarily determined by local stoichiometry. The convection term can be evaluated with unburnt and burnt velocities using first-order finite difference:

$$\mathcal{C} = \left.\frac{d(\delta V)}{dx}\right|_f = C_{\mathcal{C}} \frac{0 \cdot V_u - \delta_b \cdot V_b}{d_f} \approx -C_{\mathcal{C}} \frac{V_b}{d_f}\delta_f. \tag{14}$$

where V_u and V_b denote the fluid velocities on the unburnt and burnt sides relative to the flame front, respectively. The reaction term is approximated by the product of a rate constant and δ_f.

$$\mathcal{R} = C_{\mathcal{R}} \cdot \delta_f, \tag{15}$$

Here only destruction of δ_f is considered and hence $C_{\mathcal{R}}$ is negative. Since both convection and reaction terms are linear functions of δ_f, the model equation for δ_f can be simplified as

$$\frac{d\delta_f}{dt} = -C_{grad} \cdot f(\phi)\left.\frac{d\phi}{dx}\right|_f - C_{rlx} \cdot \delta_f, \tag{16}$$

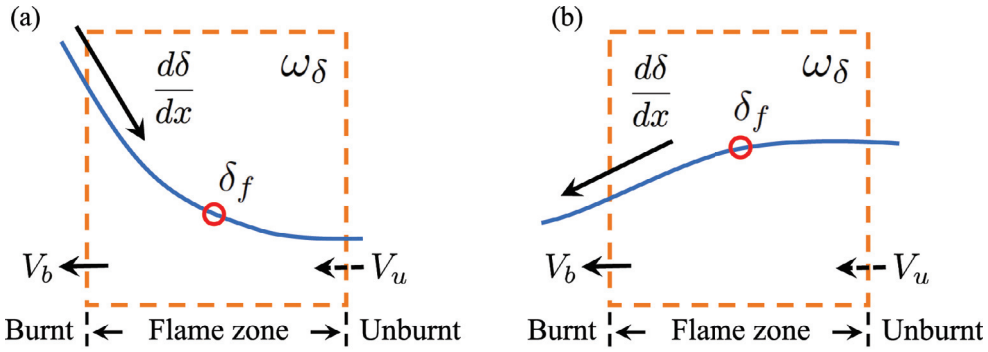

Fig. 18. Control volume analysis of Local Stratification Level (LSL): (a) stratified flame propagation along negative equivalence ratio gradient, e.g., from rich to lean; (b) stratified flame propagation along positive equivalence ratio gradient, e.g., from lean to rich.

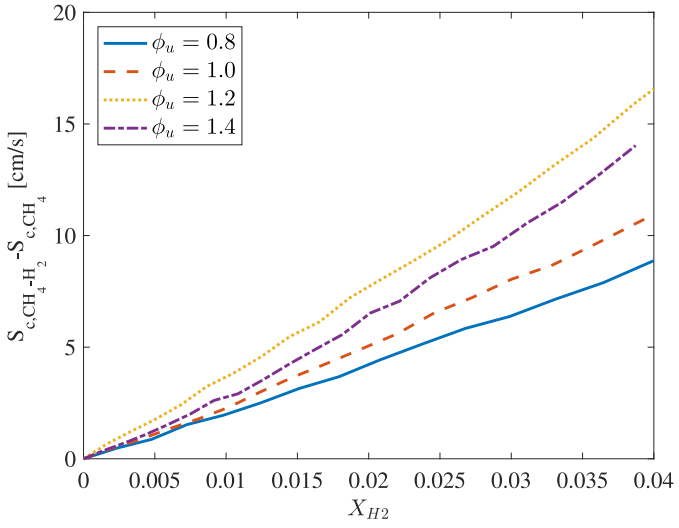

Fig. 19. Increases of laminar flame speeds with hydrogen addition to methane/air mixtures.

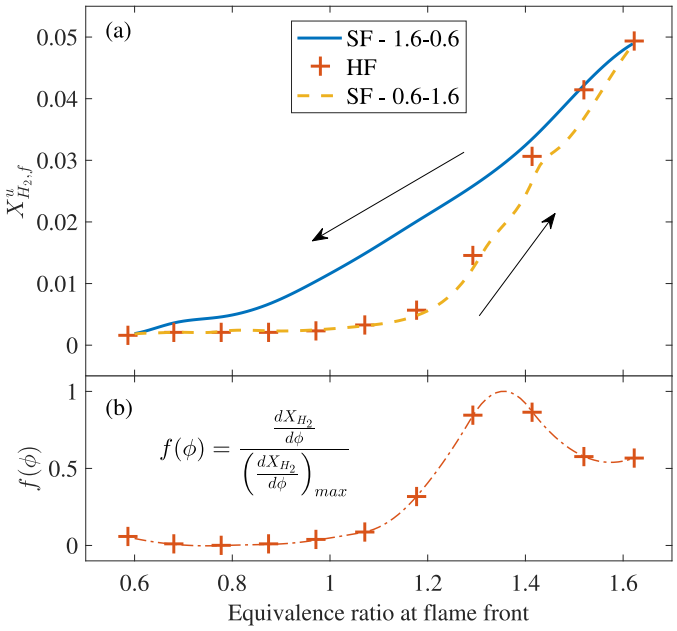

Fig. 20. (a) Mole fraction of H_2 on the unburnt side of flame front, of 1.6–0.6 SF, HF and 0.6–1.6 SF. (b) Transfer function of equivalence ratio gradient based on $X^u_{H_2,f}$ in HF.

where C_{grad} is the gradient constant and C_{rlx} the relaxation constant. The first term can be a source/sink of δ_f depending on the sign of the equivalence ratio gradient at flame front and the second term is a relaxation term. When the equivalence ratio gradient becomes zero, δ_f will relax to zero with a characteristic time scale of C_{rlx}.

During Step 2, δ_f is translated into flame speed difference between SF and HF so that stratified flame speed can be estimated as

$$S^M_{c,SF} = S^Q_{c,HF} + F(\delta_f), \tag{17}$$

where $S^Q_{c,HF}$ is the flame speed of corresponding HF based on the equivalence ratio at the flame front. Figure 17 suggests that a roughly linear relationship between flame speed difference and H_2 mole fraction difference. In addition, a set of homogeneous flame simulations is conducted where hydrogen is added to the initial unburnt mixtures of methane/air at various equivalence ratios. The results are presented in Fig. 19 showing a nearly linear relationship between the amount of hydrogen in the mixture and the increase in the flame speeds. Therefore, $F(\delta_f)$ is approximated as a linear function of δ_f:

$$F(\delta_f) = C_F \cdot \delta_f, \tag{18}$$

where C_F is defined as a scale constant of the model.

To complete the model, $f(\phi)$, C_{grad}, C_{rlx} and C_F are to be determined. Figure 20(a) shows $X^u_{H_2,f}$ versus equivalence ratios at the flame front for three flames, 1.6–0.6 SF, HF, and 0.6–1.6 SF. In Fig. 20(a), for the homogeneous flames, H_2 only exists in rich flames and increases with equivalence ratio. When the stratified flame propagates from a rich mixture to a lean mixture (1.6–0.6), the amount of H_2 increases substantially. In contrast, the amount of H_2 in 0.6–1.6 SF experiences a small decrease compared to HF. This trend is consistent with what has been observed in flame speeds of these three flames. There are two major reasons for the trend seen in the 0.6–1.6 SF. First, instead of receiving extra hydrogen from the burnt side, the lean-to-rich stratified flames at the flame front lose hydrogen to the burnt products. Second, since the temperature at flame front is lower than that of burnt products, the diffusion process along the direction from flame front to burnt product, e.g., in the 1.6–0.6 case, is promoted due to enhanced mass diffusivity in burnt gases, as well as due to the Soret effect. In comparison, the diffusion along the opposite direction, e.g., in the 0.6–1.6 case, is impeded.

The normalized H_2 gradient with respect to equivalence ratio is proposed as $f(\phi)$ and shown in Fig. 20(b), which is calculated from the HF results shown in Fig. 20(a). A 9th-order polynomial fitting of $f(\phi)$ is provided in the supplemental materials. The values of C_{grad}, C_{rlx} and C_F are first estimated from simulation results of ho-

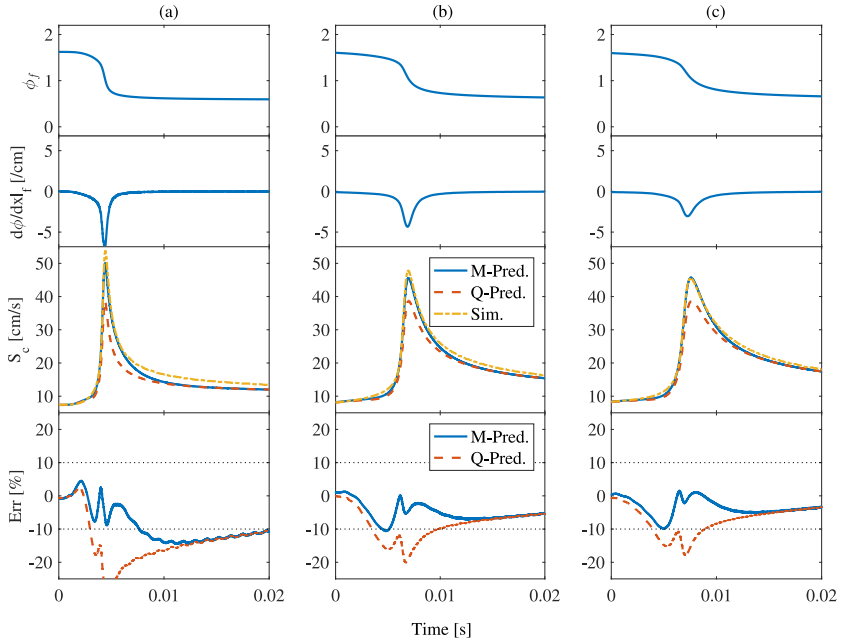

Fig. 21. LSL model assessment – three stratification cases are tested: (a) rich-to-lean, $d_s = O(0.05$ cm), (b) rich-to-lean, $d_s = O(0.1$ cm), (c) rich-to-lean, $d_s = O(1$ cm). The results are presented versus time, from top to bottom: (1) equivalence ratio at flame front, (2) equivalence ratio gradient at flame front, (3) fuel consumption speeds of model, Quasi-HF and simulation results, and (4) percentage errors of model vs. simulation and Quasi-HF vs. simulation.

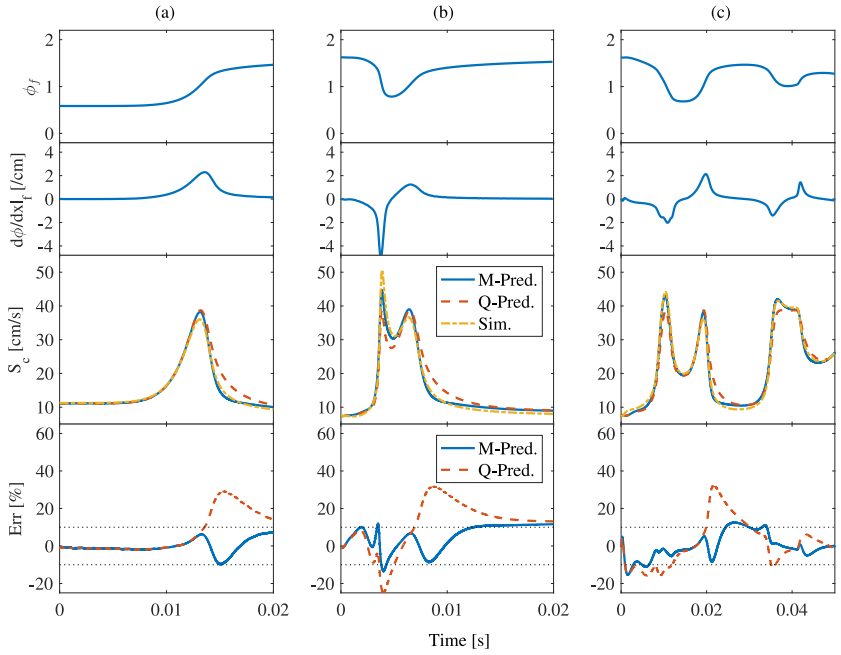

Fig. 22. LSL model assessment – three stratification cases are tested: (a) lean-to-rich, (b) rich-lean-rich, (c) arbitrary equivalence ratio profile. The results are plotted against time, from top to bottom: (1) equivalence ratio at flame front, (2) equivalence ratio gradient at flame front, (3) fuel consumption speeds of model, Quasi-HF and simulation results, and (4) percentage errors of model vs. simulation and Quasi-HF vs. simulation.

mogeneous flames. Second, to improve the accuracy of the model, these values are optimized by minimizing errors between model predictions and simulation results among all the stratified flame cases investigated in this study. The final results are shown below:

$$C_{grad} = 1.2 \times 10^3 \text{ cm} \cdot \text{s}^{-1}, \tag{19}$$

$$C_{rlx} = 8.0 \times 10^2 \text{ s}^{-1}, \tag{20}$$

$$C_F = 40 \text{ cm} \cdot \text{s}^{-1}. \tag{21}$$

The performance of the proposed model is assessed by comparisons of results for various stratification configurations. Figure 21 shows three rich-to-lean SF (1.6–0.6) cases with different stratification thicknesses, while Fig. 22 shows lean-to-rich (0.6–1.6) case, rich-lean-rich case (1.6–0.6-1.6) and a case with an arbitrary equivalence ratio profile. Both profiles of instantaneous local equivalence ratio and equivalence ratio gradient at flame front are plotted. To evaluate the model performance, the modeled stratified flame speeds (M-Pred., $S^M_{c,SF}$) and the Quasi-HF flame speeds

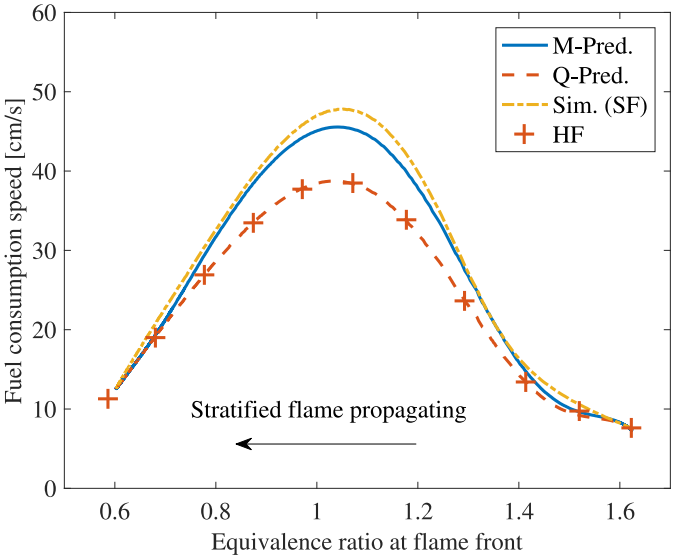

Fig. 23. Local stratification level model assessment of the rich-to-lean stratified flame, $d_s = O(0.1$ cm). The results are plotted against local equivalence ratio.

(Q-Pred., $S^{Q}_{c,HF}$) are plotted against the transient simulation results (Sim.). In the model, $F(\delta_f)$ are calculated from instantaneous equivalence ratio gradient profiles post-processed from the simulation results. Both the flame speeds and the relative errors are reported. As seen in Figs. 21 and22, for all six cases, the model results match the simulation results quantitatively: According to the direct flame speed comparisons, .i.e, the plots in the third row of both figures, the model results are seen to follow closely to those from the simulations, while the Quasi-HF approximation sometimes deviates substantially from the simulations during and after the propagation through the stratification layers. The plots in the fourth row compares the errors revealing that most errors between model predictions and simulation results are within $\sim$ 10%, which are much improved over the Quasi-HF approximations. Moreover, large departures are observed between Quasi-HF values and simulation results at locations with large degree of stratification. These comparisons suggest that the flame speeds of stratified mixtures are not accurately described by local equivalence ratio alone and a model, such as the LSL model, is necessary.

Alternatively, for SF cases with monotonic equivalence ratio profiles, the model assessment can be conducted by comparisons of flame speeds against local equivalence ratio. Figure 23 presents such a comparison for the rich-to-lean SF case with stratification thickness of 0.1 cm, i.e., the same case as shown in Fig. 21(b). Clearly, the LSL model achieve a good agreement with the simulation results. Additional model assessment with flame speeds against local equivalence ratio for cases shown in Fig. 21(a), (c) and Fig. 22(a) are provided in the supplemental materials.

The LSL model certainly can be further improved in many areas. For example, there are two assumptions made in order to treat C_{grad} and C_{rlx} as constants:

1. Both constants are independent of local equivalence ratio.
2. The relation between LSL and the difference between SF and HF is linear.

Both assumptions can be relaxed by choosing variable C_{grad} and C_{rlx} based on flame properties, such as flame thickness, characteristic velocities, of homogeneous flames. In addition, the flame stretching effect is not considered in the current planar one-dimensional simulations and it is a subject of future research.

Similar to the sensitivity analysis, the model methodology can also be applied to heavier fuel species or different diluent scenarios. However, rich flames of heavier hydrocarbon fuels still remain a challenge due to much more complicated chemical kinetics. Therefore, identification of dominant chemical and transport processes is a prerequisite to building such a model for heavier fuels.

5. Conclusions

Numerical simulations of various stratified methane/air flames are conducted and the results are analyzed by examining detailed flame properties to better understand the differences between laminar flame speeds of SF and HF. The following conclusions are drawn:

1. Among all methane/air stratified flames with different stratification configurations, rich-to-lean stratified flames show significant departures from homogeneous flames, where fuel consumption speeds of such stratified flames are up to 50% higher than those of homogeneous flames. A sensitivity analysis using the assumptions of unity Lewis number reveals that preferential diffusion of molecular hydrogen as well as H and OH is mostly responsible for such departures. On one hand, excess molecular hydrogen generates radicals H, OH and increases the reaction rates within the flame zone. On the other hand, molecular hydrogen carrying excess enthalpy increases the temperature of unburnt mixtures. Furthermore, a sensitivity analysis of H_2 and H_2O diffusivity suggests that preferential diffusion of molecular hydrogen correlates with flame speed enhancement in stratified flames, while preferential diffusion of H_2O shows an opposite effect.
2. A smaller stratification thickness leads to higher degree of departure of stratified flames from homogeneous flames. Similar trends are observed with instantaneous equivalence ratio gradients in simple stratified flames. However, both of these correlations do not include the memory effect and may not be accurate to describe stratified flames with arbitrary stratification configurations.
3. A transit Local Stratification Level (LSL) model is proposed for modeling stratified flames with arbitrary stratification configurations. The local stratification level is constructed to mimic the differences in molecular hydrogen concentration within the flame zone between SF and HF. This incorporates the effect of preferential diffusion by establishing a transfer function from molecular hydrogen concentration gradient to equivalence ratio gradient at flame front. The model results agree with those from the direct simulations with relative errors less than 10%. Potential improvements of this model may be made by adopting variable coefficients incorporating flame properties.

Acknowledgments

This work was supported by the National Science Foundation and U.S. Department of Energy under award CBET-1258653. The authors thank Professor Zheng Chen at Peking University for providing the numerical solver A-SURF.

Supplementary material

Supplementary material associated with this article can be found, in the online version, at 10.1016/j.combustflame.2017.06.010.

References

[1] A.M. Gill, S.L. Stephens, G.J. Cary, The worldwide wildfire problem, Ecol. Appl. 23 (2) (2013) 438–454.
[2] H. Phillips, Flame in a buoyant methane layer, Symp. (Int.) Combust. 10 (1) (1965) 1277–1283.
[3] J.S. Newman, Experimental evaluation of fire-induced stratification, Combust. Flame 57 (1) (1984) 33–39.

[4] M. Sjöberg, J. Dec, Smoothing HCCI Heat-Release Rates Using Partial Fuel Stratification with Two-Stage Ignition Fuels, SAE Technical Paper 2006-01-0629, 2006, doi:10.4271/2006-01-0629.
[5] R.D. Reitz, Directions in internal combustion engine research, Combust. Flame 160 (2013) 1–8.
[6] H. Ax, W. Meier, Experimental investigation of the response of laminar premixed flames to equivalence ratio oscillations, Combust. Flame 167 (2016) 172–183.
[7] S. Candel, Combustion dynamics and control: Progress and challenges, Proc. Combust. Inst. 29 (1) (2002) 1–28.
[8] A.C. Alkidas, Combustion advancements in gasoline engines, Energy Convers. Manag. 48 (2007) 2751–2761.
[9] C. Park, S. Kim, H. Kim, Y. Moriyoshi, Stratified lean combustion characteristics of a spray-guided combustion system in a gasoline direct injection engine, Energy 41 (2012) 401–407.
[10] V.S. Santoro, A. Liñán, A. Gomez, Propagation of edge flames in counterflow mixing layers: experiments and theory, Proc. Combust. Inst. 28 (2) (2000) 2039–2046.
[11] G.A. Karim, P. Tsang, Flame propagation through atmospheres involving concentration gradients formed by mass transfer phenomena, J. Fluids Eng. 97 (1975) 615.
[12] O. Badr, G. Karim, Flame propagation in stratified methane-air mixtures, J. Fire Sci. 2 (1984) 415–426.
[13] D.W. Mikolaitis, The unsteady propagation of premixed flames through nonhomogeneous mixtures and thermal gradients, Combust. Flame 57 (1984) 87–94.
[14] E.J. Bissett, D.L. Reuss, Analysis of a nonadiabatic flame propagation through gradients of fuel or temperature, Symp. (Int.) Combust. (1986) 531–538.
[15] T. Kang, D.C. Kyritsis, Methane flame propagation in compositionally stratifid gases, Combust. Sci. Technol. 177 (2005) 2191–2210.
[16] T. Kang, D.C. Kyritsis, Departure from quasi-homogeneity during laminar flame propagation in lean, compositionally stratified methane-air mixtures, Proc. Combust. Inst. 31 (2007) 1075–1083.
[17] T. Kang, D.C. Kyritsis, Theoretical investigation of flame propagation through compositionally stratified methane-air mixtures, Combust. Theor. Model. 13 (2009) 705–719.
[18] S. Balusamy, A. Cessou, B. Lecordier, Laminar propagation of lean premixed flames ignited in stratified mixture, Combust. Flame 161 (2014) 427–437.
[19] R.A. Owston, Modeling of combustion in stratified hydrogen-air mixtures, Purdue University, 2010 Ph.D. thesis.
[20] J. Zhang, J. Abraham, A numerical study of laminar flames propagating in stratified mixtures, Combust. Flame 163 (2016) 461–471.
[21] X. Shi, J.-Y. Chen, Y. Chen, Laminar flame speeds of stratified methane, propane, and n-heptane flames, Combust. Flame 176 (2017) 38–47.
[22] X. Shi, J.-Y. Chen, Z. Chen, Numerical study of laminar flame speed of fuel-stratified hydrogen/air flames, Combust. Flame 163 (2016) 394–405.
[23] Z. Chen, M.P. Burke, Y. Ju, Effects of Lewis number and ignition energy on the determination of laminar flame speed using propagating spherical flames, Proc. Combust. Inst. 32 (2009) 1253–1260.
[24] Z. Chen, Effects of radiation and compression on propagating spherical flames of methane/air mixtures near the lean flammability limit, Combust. Flame 157 (2010) 2267–2276.
[25] R. Kee, J. Warnatz, J. Miller, A fortran computer code package for the evaluation of gas-phase viscosities, conductivities, and diffusion coefficients, Report No. SAND83-8209, Sandia National Laboratories, Livermore, CA, USA, 1983.
[26] R.J. Kee, F. Rupley, E. Meeks, J. Miller, CHEMKIN-III: A fortran chemical kinetics package for the analysis of gas-phase chemical and plasma kinetics, Report No. SAND96-8216, Sandia National Laboratories, Livermore, CA, USA, 1996.
[27] G.P. Smith, D.M. Golden, M. Frenklach, N.W. Moriarty, B. Eiteneer, M. Goldenberg, C.T. Bowman, R.K. Hanson, S. Song, J. William C. Gardiner, V.V. Lissianski, Z. Qin, GRI-Mech 3.0, 1999. http://www.me.berkeley.edu/grimech.
[28] T. Poinsot, T. Echekki, M.G. Mungal, A study of the laminar flame tip and implications for premixed turbulent combustion, Combust. Sci. Technol. 81 (1992) 45–73.
[29] C. Law, C. Sung, Structure, aerodynamics, and geometry of premixed flamelets, Prog. Energy Combust. Sci. 26 (2000) 459–505.
[30] A.D. Cruz, A.M. Dean, J.M. Grenda, A numerical study of the laminar flame speed of stratified methane/air flames, Proc. Combust. Inst. 28 (2000) 1925–1932.
[31] P.C. Vena, B. Deschamps, G.J. Smallwood, M.R. Johnson, Equivalence ratio gradient effects on flame front topology in a stratified iso-octane/air turbulent V-flame, Proc. Combust. Inst. 33 (2011) 1551–1558.
[32] C. Sorensen, Measurement of flame propagation through step changes in mixture composition, Massachusetts Institute of Technology, 2016 Ph.D. thesis.
[33] N. Peters, Turbulent combustion, Cambridge University Press, 2000.